

LES and Acoustic Analysis of Turbulent Reacting Flows: Application to a 3D Oscillatory Ramjet Combustor

L.Y.M. Gicquel* , Y. Sommerer † and B. Cuenot *
CERFACS, 31057, Toulouse, France

T. Poinso†
IMFT, 31400 Toulouse, France

I. Introduction

Recent numerical predictions of turbulent reacting flows obtained by Large Eddy Simulations (LES)¹⁻⁶ underline the power of the approach for laboratory and industry like configurations. Based on the filtered multi-species compressible Navier-Stokes equations, LES aim at simulating large scale flow structures while modelling small scale effects. The approach henceforth offers partial representation of the temporally evolving physics involved in turbulent reacting flows. Of the known crucial mechanisms accessible to compressible LES, one retains: acoustics/flame interactions, hydrodynamic instabilities/flame interactions, time dependent mixing processes...

Most recent LES focus on gas turbine configurations because these systems exhibit a variety of difficult problems: Ignition, quenching, instabilities for which LES is a logical path since the end of the 90's. Ramjet burners receive less attention since the pioneering work of Kailasanath *et al.*,⁷ Menon *et al.*⁸ and only few studies are devoted specifically to LES of ramjets.⁹⁻¹¹ In the present work, the LES tools used recently for gas turbine flows^{1,2} are applied to a ramjet configuration. This type of combustor exhibits significant differences compared to gas turbine flows: the velocities are much higher, combustion is not stabilised by swirl, a choked nozzle usually terminates the chamber.

As a first assessment of LES in this context of high speed reacting flow combustors, LES results are compared to turbulent reacting and non-reacting experimental measurements.^{12, 13} Among the simulated combustion regimes, the higher equivalence ratio is found to be self-oscillatory when simulated by LES. Temporal analyses of the instantaneous LES results obtained for an equivalent ratio of 0.75 indicate the presence of acoustic waves independently of the boundary conditions imposed at the inlet. These waves are generated in the impingement zone of the jets and propagate toward the inlets, the head-end of the chamber and the choked nozzle. The frequency ($\approx 8,000$ Hz) matches the first acoustic transverse mode of the main duct and is very similar to high frequency modes called "screech" identified in laboratory burners¹⁴ or gas turbines.¹⁵

Prior to the presentation of the geometry, the description of the computational domain and the boundary conditions, a brief overview of the LES governing equations and models used in this work is given. The result section is dedicated to the presentation of the cold and reacting flow simulations. Details of the flow topology are given at this occasion followed by the comparison of the time averaged LES results against experimental data. Finally, the oscillatory reacting case obtained with LES is described in term of acoustic/pressure fields.

*Senior Researcher, CFD Combustion Team, 42 Av. G. Coriolis.

†Researcher Engineer, CFD Combustion Team, 42 Av. G. Coriolis.

‡Professor, Allée du Professeur C. Soula, and AIAA Member Grade.

II. Numerical Approach

Turbulent flows are known to contain large ranges of scales.^{16–18} These scales have been repeatedly evidenced in experimental measurements or Direct Numerical Simulations (DNS) and LES. The large scale phenomena are usually associated with vortical structures whose dimensions are of the order of the domain size. The evolution of these scales is governed by the geometry of the combustion chamber and they carry most of the turbulent kinetic energy. The smaller scales have on the other hand a relatively short range of influence and are believed to behave in a more universal way. Contrary to RANS where all scales need to be modelled, LES filters out the small universal scales and aims at simulating only the dynamics of the large scales. The modelling is eased thanks to the universality of the physics governing the small scales. It yields an approach which is flexible and well suited to simulate cases encountered in the industry where large scale phenomena are known to be very important.

A. Governing Equations

LES involves the spatial filtering operation which reduces for spatially, temporally invariant and localised filter functions,^{19, 20} to:

$$\overline{f(\mathbf{x}, t)} = \int_{-\infty}^{+\infty} f(\mathbf{x}', t) G(\mathbf{x}' - \mathbf{x}) d\mathbf{x}', \quad (1)$$

where G denotes the filter function and $\overline{f(\mathbf{x}, t)}$ is the filtered value of the variable $f(\mathbf{x}, t)$.

In the mathematical description of compressible turbulent flows with chemical reactions and species transport, the primary variables are the species volumic mass fractions $\rho_\alpha(\mathbf{x}, t)$, the velocity vector $u_i(\mathbf{x}, t)$, the total energy $E(\mathbf{x}, t) \equiv e_s + 1/2 u_i u_i$, and the density $\rho(\mathbf{x}, t) = \sum_{\alpha=1}^N \rho_\alpha(\mathbf{x}, t)$. Note that $\rho_\alpha(\mathbf{x}, t)$ is linked to the species mass fractions $Y_\alpha(\mathbf{x}, t)$ and for which mass conservation imposes for a mixture of N species: $\sum_{\alpha=1}^N Y_\alpha(\mathbf{x}, t) = 1$.

The fluid to be considered follows the ideal gas law, $p = \rho r T$ and $e_s = \int_0^T C_p dT - p/\rho$, where e_s is the mixture sensible energy, T the temperature, C_p the fluid heat capacity at constant pressure and r is the mixture gas constant. The viscous stress tensor, the heat diffusion vector and the species molecular transport use classical gradient approaches. The fluid viscosity follows Sutherland's law, the heat diffusion coefficient follows Fourier's law, and the species diffusion coefficients are obtained using a species Schmidt number along with the Hirschfelder Curtis approximation. Note that due to the last approximation, diffusion velocity corrections are added for mass conservation. Hereinafter variations of the molecular coefficients resulting from the unresolved fluctuations are neglected so that the various expressions for the molecular coefficients become only a function of the filtered field.²¹

The application of the filtering operation to the instantaneous set of compressible Navier-Stokes transport equations with chemical reactions yields the LES transport equations to be solved numerically.²¹ However and due to the non-linear character of the initial system, the so-called Sub-Grid Scale (SGS) quantities need modelling for the system to be closed.^{22, 23}

B. LES closures

The unresolved SGS stress tensor $\overline{\tau_{ij}^t}$, is usually addressed through the concept of SGS turbulent viscosity model and the Boussinesq assumption.^{24, 25} The model henceforth reads (Smagorinsky²⁶):

$$\overline{\tau_{ij}^t} - \frac{1}{3} \overline{\tau_{kk}^t} \delta_{ij} = -2 \bar{\rho} \nu_t \tilde{S}_{ij}, \quad (2)$$

with,

$$\tilde{S}_{ij} = \frac{1}{2} \left(\frac{\partial \tilde{u}_i}{\partial x_j} + \frac{\partial \tilde{u}_j}{\partial x_i} \right) - \frac{1}{3} \frac{\partial \tilde{u}_k}{\partial x_k} \delta_{ij}. \quad (3)$$

In (2) & (3) \tilde{S}_{ij} is the resolved strain tensor and ν_t is the SGS turbulent viscosity. The Smagorinsky model²⁶ is used here. It expresses ν_t as:

$$\nu_t = (C_S \Delta)^2 \|S\|. \quad (4)$$

In (4), Δ denotes the filter characteristic length and is approximated by the cubic-root of the cell volume, C_S is the model constant ($C_w = 0.18$) and $\|S\| = (2 \tilde{S}_{ij} \tilde{S}_{ij})^{1/2}$.

The SGS species flux $\overline{J}_i^{\alpha t}$ and the SGS energy flux \overline{q}_i^t are respectively modelled by use of the species SGS turbulent diffusivity $D_t^\alpha = \nu_t / Sc_t^\alpha$, where Sc_t^α is the turbulent Schmidt number ($Sc_t^\alpha = 0.7$ for all α). The eddy diffusivity is also used along with a turbulent Prandtl number $Pr_t = 0.9$, so that $\lambda_t = \bar{\rho} \nu_t C_p / Pr_t$:

$$\overline{J}_i^{\alpha t} = -\bar{\rho} \left(D_t^\alpha \frac{W_\alpha}{W} \frac{\partial \tilde{X}_\alpha}{\partial x_i} - \tilde{Y}_\alpha V_i^c \right) \quad \text{and} \quad \overline{q}_i^t = -\lambda_t \frac{\partial \tilde{T}}{\partial x_i} + \sum_{\alpha=1}^N \overline{J}_i^{\alpha t} \tilde{h}_s^\alpha. \quad (5)$$

In Eq. (5) the mixture molecular weight W and the species molecular weight W_α can be combined with the species mass fraction to yield the expression for the molar fraction of species α : $X_\alpha = Y_\alpha W / W_\alpha$. In expression (5), V_i^c is the diffusion correction velocity resulting from the Hirschfelder Curtis approximation²¹ and \tilde{T} is the modified filtered temperature which satisfies the modified filtered state equation,²⁷⁻³⁰ $\bar{p} = \bar{\rho} r \tilde{T}$. Finally, \tilde{h}_s^α stands for the enthalpy of species α . Although the performances of the closures could be improved through the use of a dynamic formulation,^{27, 31-34} they are considered sufficient to address the present investigation.

LES of turbulent reacting flows imply the modelling of SGS combustion terms. The model employed here stems from the proposition for the propagation of a premixed flame on coarse meshes. Following the theory of laminar premixed flames³⁵ the flame speed S_l^0 and the flame thickness δ_L^0 may be expressed as:

$$S_l^0 \propto \sqrt{\lambda A} \quad \text{and} \quad \delta_L^0 \propto \frac{\lambda}{S_l^0} = \sqrt{\frac{\lambda}{A}}, \quad (6)$$

where λ is the thermal diffusivity and A the pre-exponential constant. Increasing the thermal diffusivity by a factor F , the flame speed is kept unchanged if the pre-exponential factor is decreased by the same factor. It also results from this operation a flame thickness multiplied by F and easily resolved on a coarser mesh. Interaction between turbulence and chemistry is nonetheless decreased as expressed by the new Damköhler number which decreases by the factor F : The flame becomes less sensitive to the surrounding turbulent structures.

Similar reasoning can be applied to the LES set of equations and thickening of the flame can be interpreted as a step toward the full modelling of the SGS combustion quantities. Additional information needs however to be supplied so as to properly reproduce the effect of the missing interaction between turbulence and chemistry. This is the intent of the so-called efficiency function, E .³⁶ It is important to acknowledge the limitation of the reasoning to fully premixed combustion. Although real combustors rarely operate with pure diffusion flames, they cannot ensure fully premixed regimes of combustion and partially premixed regimes dominate. For accurate mixing predictions, molecular and thermal diffusions cannot be overestimated by a factor F in partially mixed zones where no combustion occurs (it would yield over-estimated mixing and wrong flame positioning). In reacting zones, diffusion and source terms issued from the thickened reaction are well resolved and turbulence should be solely represented by the efficiency function, E . Dynamic thickening is introduced to account for these two points.²¹

The final expressions of the SGS combustion models read:

$$\overline{J}_i^{\alpha t} = (1 - S) \bar{\rho} D_t^\alpha \frac{W_\alpha}{W} \frac{\partial \tilde{X}_\alpha}{\partial x_i} + \bar{\rho} \tilde{Y}_\alpha V_i^c \quad \text{and} \quad \overline{q}_i^t = (1 - S) \lambda_t \frac{\partial \tilde{T}}{\partial x_i} + \sum_{\alpha=1}^N \overline{J}_i^{\alpha t} \tilde{h}_s^\alpha. \quad (7)$$

where V_i^c is obtained as usual and includes the correction coefficient $(1 - S)$. In Eq. (7), S is the local sensor depending on the local temperature and mass fractions,

$$S = \tanh(\beta' \frac{\Omega}{\Omega_0}) \quad \text{and} \quad \Omega = Y_F^{\nu'_F} Y_O^{\nu'_O} \exp(-\Gamma \frac{E_a}{RT}). \quad (8)$$

$\Gamma = 0.5$ ensures that thickening appears before the reaction front, while $\beta' = 500$ controls the slope of the test function. The thickening function is in this work obtained from the local grid resolution and ensures that the flame front is resolved on a given number of grid points ($N_c = 5$ for all computations presented in this work):

$$F = 1 + (F_{max} - 1)S \quad \text{and} \quad F_{max} = \frac{N_c}{\Delta_x} \delta_L^0. \quad (9)$$

Despite the lack of theoretical validation of the proposed combustion models for partially-premixed and diffusion flames, its ease of implementation and prior applications^{1,2} assert its suitability for the problem addressed in this work.

III. Simulations

Assessment of LES in the context of high speed flows is performed for a laboratory ramjet configuration.

Although simplified for experimental purposes, the retained configuration is composed of all the geometrical characteristics encountered in a real dump ramjet combustion chamber.

A. Flow configurations

The main chamber is 1260 mm long and consists of a closed square duct (of 160 mm sides) which terminates by a choked nozzle. Air flows in the chamber through two intakes of square cross section (of 80 mm sides) angled at $\Pi/4$ radians with the main chamber's axis and positioned on the top and bottom floors of the main duct. These intakes are connected to the chamber 50 mm away from the main duct end-wall yielding a geometrical dead zone usually referred as the head-end or dome of the device. For the reacting cases, two jets feed gaseous propane to the head-end of the chamber. These jets are located on the end-wall of the ramjet combustor, Fig. 3, and are inactive for the cold flow set-up.

Three cases are considered for the simulations: one non-reacting and two reacting flows. The operating conditions are given in Table. 1 and are all obtained with an inflow air mass flow of 0.9 kg/s. Measurements are obtained for the three conditions and obtained through various techniques. Data consists in cross-stream and spane-wise velocity profiles obtained at various downstream locations along the main pipe. Details on the experimental apparatus and rig are available in A. Ristori *et al.*¹² and C. Brossard *et al.*¹³

Table 1. Operating conditions considered for LES.

Flow configuration	Equivalence ratio: Φ
Non-reacting	NA
Reacting	0.5
Reacting	0.75

B. Computational aspects

The computational domain considered for LES treats the entire combustion chamber: the head-end with the propane injection, the air intakes with square cross sections and a choked nozzle prior to the exit. The

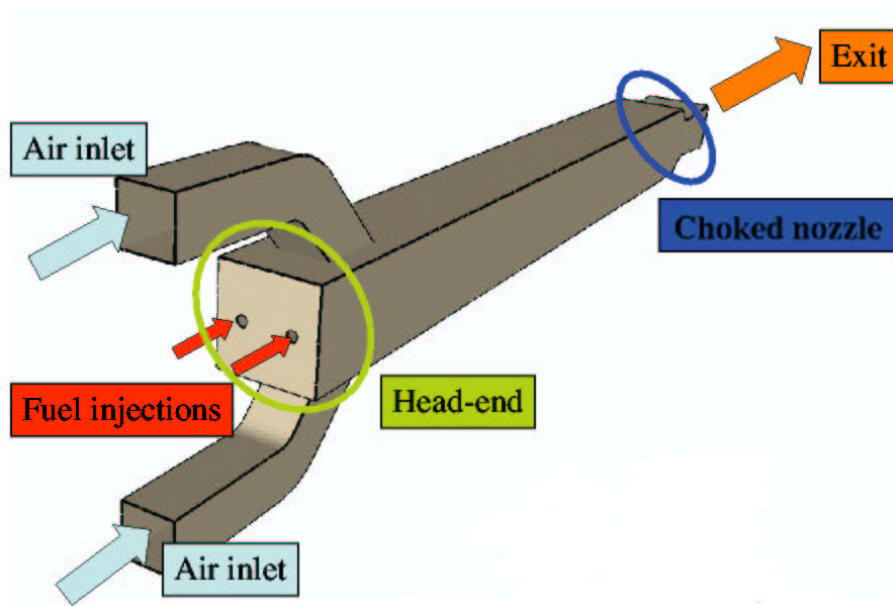


Figure 1. Ramjet configuration as studied experimentally.

fully unstructured mesh is composed of 1,173,736 tetrahedra. Mesh refinement is enforced in the region of potential flame locations as well as zones of turbulence generation and large velocity gradients, Fig. 3. A one-step chemistry scheme for propane derived from a detailed mechanism (GRI-Mech-III) is employed along with the dynamic thickened flame approach for LES combustion modelling. Turbulent LES closure makes use of the conventional Smagorinsky model.²⁶ Walls are treated as adiabatic and inlet profiles satisfy the flow rates measured on the experimental test rig. Note that all inlet conditions are characteristic based and make use of the Navier-Stokes Characteristic Boundary Conditions which allow a proper control of acoustic behaviour of the inlet. Finally, the exit condition is supersonic (choked nozzle) so that no particular treatment at the boundary is necessary since it is a numerically and theoretically well defined condition.

IV. Results

Application of the previously described methodology to ramjet reacting flows is exposed in this section.

Specific attention is devoted to the validation of LES against experimental data. Once validated the approach is utilised to simulate a second reacting regime which proves to be self-oscillatory: Apparition of a strongly periodic evolution of the system while combustng. Prior to the validation of the method, general topological aspects as obtained from LES are first highlighted for the cold flow predictions. Prominent structures are evidenced and their importance and impact on the reacting flows are underlined. The assessment of the LES predictions is then obtained in term of Reynolds averaged solutions and by comparisons against corresponding experimental results. To conclude, the unsteady behaviour of the oscillatory ramjet regime is illustrated and discussed.

A. Flow topology

Ramjet combustors differ from conventional air breathing engines by the velocity levels encountered in the former configuration. While the latter essentially rely on swirl and low velocity regions to facilitate

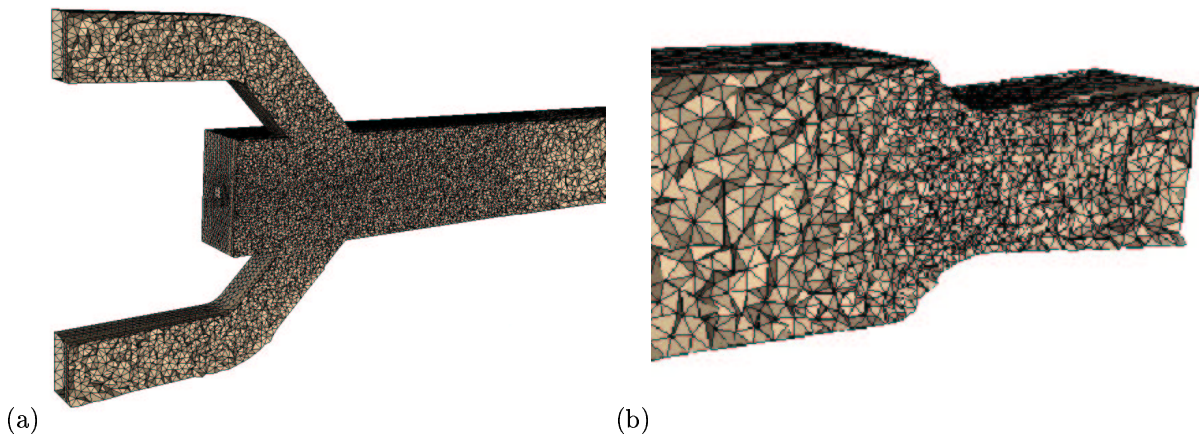


Figure 2. Typical view of the grid considered for LES of the cold and reacting flows: (a) expected region of fuel consumption and (b) choked nozzle. Only half of the domain is illustrated for clarity.

premixing and combustion, the former operates with velocity levels often incompatible with flame speeds as obtained in fully or partially premixed combustion. Ramjet combustors are hence often found to burn in diffusive regimes for which the fuel consumption rate essentially depends on the mixing process taking place between the high speed air stream and the injected fuel. Understanding of the flow structures is in that context critical to properly simulate high speed combustor reacting flows. Prior to the fully reacting LES cases, cold flow simulations are presented below. The aim of this initial section is to acquaint the reader with flow structures as encountered in this type of configuration. No specific validation is intended at this stage, only flow topology is presented and as obtained from the cold LES predictions.

Preliminary analysis and visualisation of the predictions obtained for the non-reacting ramjet reveal distinct flow regions in the chamber. Three zones appear to be critical for the stabilisation, mixing and stability of the combustor flow. Fig. 3 identifies the three flow structures observed in the LES and visualised by use of isosurfaces of positive and negative axial components of the velocity vector and a Q -criterion isosurface.³⁷ The main region of influence depicted on Fig. 3 by the red isosurface (positive value of the axial velocity component) derives from the air streams issued from the top and bottom air intakes. As these two streams enter the main duct chamber the potential core of each jet strongly impact each other generating a large sheet of fluid with high values of axial velocity. Travelling further downstream the high speed flow sheet impacts the chamber side walls before slowing down further downstream. Such a flow structure is classical of impacting jet flows and is known to generate oscillations. The second region identified by the blue isosurface for negative values of the axial velocity component indicates back flow regions in the head-end of the ramjet. Finally four corner vortices (yellow isosurfaces) connect the head-end of the ramjet with the rest of the chamber. The apparition of such structures is essentially explained by the lateral sudden expansion seen by the high speed jets issuing from the air stream intakes and generating strong re-circulating flows at these four locations.

The first region is expected to oscillate which should have a strong impact on the flame stabilisation. Likewise, back flow from the jet air toward the head-end where fuel is injected eases premixing of the air/fuel mixture prior to its combustion. Finally corner vortices contribute to the generation of low velocity regions allowing flame stabilisation and flame anchoring zones while in a high speed flow regime.

Extension to the reacting flow ($\Phi = 0.5$, Table. 1) confirms the previous findings as illustrated on Fig. 4. Based on instantaneous LES fields, Fig. 4(a), the flame anchors itself in regions of low velocity around the

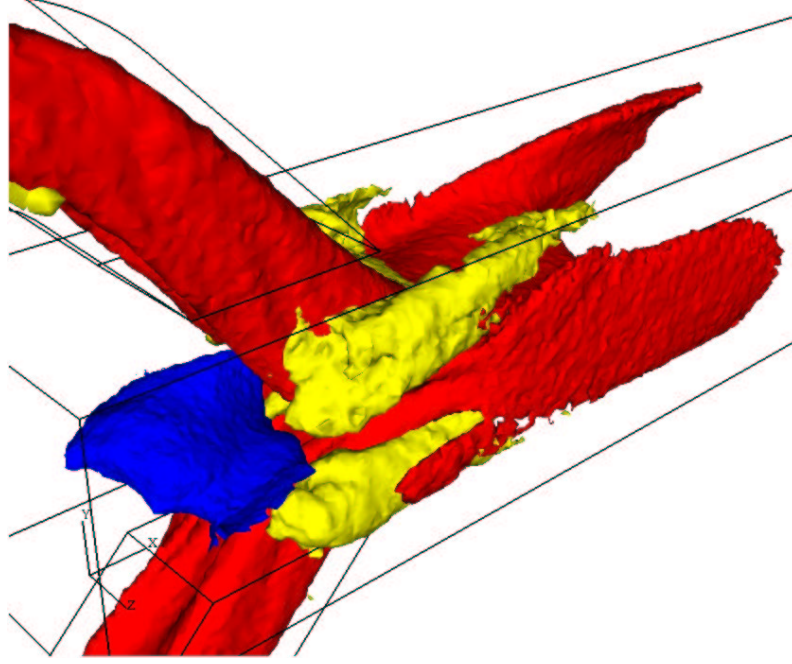


Figure 3. Flow structures as evidenced from the cold flow LES, Table. 1. Isosurfaces illustrate the extent of the various regions: positive / negative values of the stream-wise velocity component for the red / blue surfaces, while yellow surfaces stem from the Q-criterion³⁷ and highlight the presence of corner vortices.

jet interaction region, Fig. 3. Construction of the Takeno index, turquoise green isosurface on Fig. 4, corroborates the previous observation and demonstrates the tendency for the flame to burn in a diffusion regime for a good length of the chamber. Resulting from this regime are very high temperature spots travelling downstream the main pipe. High fuel concentrations are restricted to the head-end region as observed by the grey isosurface ($Y_{\text{fuel}} = 0.9$) and where it rapidly mixes with the re-circulating air coming from the main jets. A fuel isosurface coloured by the heat release intensity is shown on Fig. 4(b), $Y_{\text{fuel}} = 0.6$. Based on this criterion, the fuel mixture essentially propagates between the jets, the corner vortices and the high velocity fluid impacting the side walls of the chamber. Combustion concentrates to low velocity regions where fuel meets air at the stoichiometric ratio.

Investigations of the instantaneous LES fields obtained for the non-reacting and the reacting cases emphasise the impact of the flow topology. The ramjet under investigation exhibits distinct flow behaviours which are found to differ only slightly for the reacting and the cold flow results (at least for the operating conditions presented). Proper prediction of the flow structure henceforth guaranties good level of predictions of the reacting flows emphasising the importance of mixing for this high speed flow configuration. Clear assessment of the predictions obtained numerically is however still needed at this point and is the aim of the following section.

B. LES validation: $\Phi = 0.5$

Prior to the application of the method to a wide range of operating conditions of the ramjet combustion chamber, a clear evaluation of the LES results is obtained through comparisons against experimental measurements. Time averaged LES profiles result from an unsteady reacting LES ($\Phi = 0.5$) running over five convective times. Convergence of the mean statistical field is ensured at the first means and the fluctuating levels. Profiles of the velocity field are taken at various stream-wise locations in the main duct

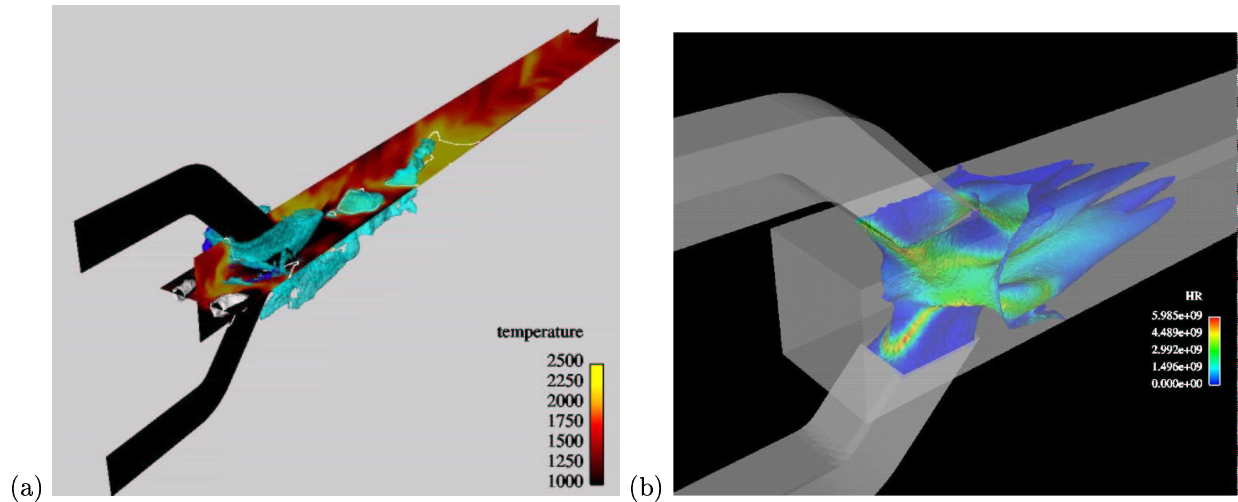


Figure 4. Flow structures as evidenced from the reacting flow LES $\Phi = 0.5$, Table. 1.

chamber and along the two symmetry planes ($y = 0$ and $z = 0$).

Experimental data^{12,13} consists in velocity profiles obtained from two particle tracing techniques. The first approach uses soot particles issued by the chemical reaction, while the second method makes use of Magnesium particle seeds. Both techniques have inherent uncertainties which remain difficult to circumvent especially for the flow configuration under study. The data-basis is nonetheless a very valuable tool to gauge LES results.

Figure. 5 presents the comparisons between experiments and LES. Transverse profiles, Fig. 5(a), indicate the overall good agreement of the LES predictions with the experiment. Jet trajectories and penetrations within the combustion chamber are well reproduced although stream-wise velocity amplitudes are usually slightly over-estimated. Re-circulation of the jet air in the head-end of the combustor seems over-estimated while transverse components of the velocity vector are in good agreement with the measures. Cross-stream profiles, Fig. 5(b), confirm the general quality of the LES results. Re-circulation regions are well reproduced and velocity levels are within experimental uncertainties.

General agreement between experiments and reacting LES predictions is very satisfactory and underlines the potential of the method in reproducing high speed reacting flows. Flow structures are very well reproduced by the numeric which usually falls within experimental uncertainties. It is important to emphasise at this point the potential improvements necessary for LES of such configurations. First, wall treatment was found to be critical. Second, compressibility effects and combustion modelling will understandably play major roles for such reacting flows. Improvement of the modelling necessary by LES can henceforth only improve the general quality of the predictions as obtained here and which relied on previous developments as usually applied in conventional gas turbine LES applications. Although limited the models developed previously seem to yield very good results and constitute a very encouraging basis for further developments.

C. Oscillatory LES predictions: $\Phi = 0.75$

Once validated, reacting LES is applied to the same ramjet geometry but for the second regime, Table. 1. The motivation for this computation originates from the observation that around the target equivalence ratio the experimental rig is found to transition to a noisy type of combustion with a pronounced acoustic tone corresponding to the so called "screech" mode found in laboratory burners¹⁴ or gas turbines.¹⁵ Prospective LES are in this context very interesting to further assess the potential of the approach.

Unsteady LES predictions obtained for $\Phi = 0.75$ evidenced a strong periodic phenomenon in term of heat release, pressure fluctuations and turbulent kinetic energy of the system. Visualisation of the pressure field in the vertical symmetry plane, Fig. 6, clearly puts light on the source the periodic phenomenon. Pressure contours, depicted for a full cycle of the unsteadiness, seems to exhibit an oscillating source located near the aft section of the two impacting air jets. Pressure waves radiating from the source trigger planar waves when hitting the top and bottom edges of the air intakes. These waves then travel up-stream the air intakes before exiting the computational through the main air inlets. *A posteriori* analysis of the reflection coefficient of the air inlet boundary condition proved to be very small ensuring the characteristic treatment not to be the feeding source of the oscillation which therefore seem self sustained.

Acoustic analysis of the chamber yields eigen-frequencies. Among all the possible eigen-modes, the first transverse acoustic mode ($\approx 8,000$ Hz) concurs with the observed self-sustained source oscillation. Further acoustic analysis of the LES results is however needed to properly identify the origin for such an oscillatory behaviour to occur. Preliminary observations still remain very valuable and demonstrate the power of LES for the prediction of turbulent reacting flows.

V. Conclusion

Large eddy simulations of turbulent reacting flows are assessed for its application to ramjet combustors. Although derived initially for low velocity partially premixed flows such as encountered in conventional gas turbine engines and aeronautical combustion chambers, preliminary results are very encouraging. Gauging against experimental measures ensures that mean flow features are well captured and mean velocity profiles are found to be in good agreement with experimental data obtained for the test configuration. Extension to a higher equivalence ratio regime yields numerical predictions that are unstable and where acoustic seems to play an important role. Further investigations on the mechanisms involved in this self excited reacting flow are however still needed.

Acknowledgments

The authors gratefully acknowledge the implication of MBDA for its support as well as the "Centre Informatique National de l'Enseignement Supérieur" (CINES) located at Montpellier, France for computer access to its facility.

References

- ¹L. Selle *et al.*, *Compressible Large-Eddy Simulation of turbulent combustion in complex geometry on unstructured meshes*, Combustion and Flame, **137**, 4, pp.489–505, 2004.
- ²S. Roux *et al.*, *Studies of mean and unsteady flow in a swirled combustor using experiments, acoustic analysis and Large Eddy Simulations*, Combustion and Flame, in press, 2005.
- ³V. Sankaran *et al.*, *LES of Spray Combustion in Swirling Flows*, Journal of Turbulence, Vol. 3, No 2, 2002.
- ⁴H. Pitsch *et al.*, *Flamelet modeling of non-premixed turbulent combustion with local extinction and re-ignition*, Comb. Theory Modelling, 2002.
- ⁵Y. Sommerer *et al.*, *Large eddy simulation and experimental study of flashback and blow-off in a lean partially premixed swirled burner*, Journal of Turbulence, 5:037, 2004.
- ⁶C. Prire *et al.*, *Experimental and numerical studies of dilution systems for low emission combustors*. AIAA Journal, 43(8):1753-1766, 2005.
- ⁷K. Kailasanath *et al.*, *Effects of Energy Release on High Speed Flows in an Axisymmetric Combustor*, AIAA-89-0385, 1989.
- ⁸S. Menon *et al.*, *Simulations of Ramjet Combustor Flow Fields Part I - Numerical Model, Large-Scale and Mean Motions*, AIAA-87-1421, 1987.
- ⁹Menon *et al.*, *Large-Eddy Simulations of Combustion Instability in An Axisymmetric Ramjet Combustor*, AIAA-90-0267, 1990.
- ¹⁰Samaniego *et al.*, *Low-Frequency Combustion Instability Mechanisms in a Side-Dump Combustor*, Combustion and Flame, 94:363-380, 1993.

- ¹¹Dufour *et al.*, *Numerical Simulation of Direct Connect Liquid-Fueled Ramjet Tests*, AIAA-98-3769, 1998.
- ¹²A. Ristori *et al.*, *Research ramjet program: an initiative to improve knowledge on ramjet reactive flowfields*, 4th ONERA/DLR Aerospace Symposium, TP- 2004-01, 13-14 June, Koln. Germany, 2002.
- ¹³C. Brossard *et al.*, *Caractérisation par vélocimétrie laser de l'écoulement dans un foyer maquette de statoréacteur*, 8ème Congrès Francophone de Vélocimétrie Laser, TP- 2002-29, 17-20 Septembre, Orsay. France, 2002.
- ¹⁴Don E. Rogers *et al.*, *A Mechanism for High-Frequency Oscillation in Ramjet Combustors and Afterburners*, Jet Propulsion, 456-462, 1956.
- ¹⁵S. Rea *et al.*, *On-line combustion monitoring on dry low NOx industrial gas turbines*, Meas. Sci. Technol., **14**, 1123-1130, 2003.
- ¹⁶Batchelor, G. K., *The theory of Homogeneous Turbulence*, Cambridge, University press, 1967.
- ¹⁷Tennekes *et al.*, *A First Course in Turbulence*, The MIT press, 1972.
- ¹⁸Hinze, J. O., *Turbulence*, McGraw-Hill Series in Mechanical Engineering, 1975.
- ¹⁹Aldama, A. A., *Filtering Techniques for Turbulent Flow Simulations*, New York, Springer, 1990.
- ²⁰Vreman, B., Geurts, B., and Kuerten, H., *Realizability conditions for the turbulent stree tensor in large-eddy simulation*, Journal of Fluid Mechanics, Vol. 278, pp. 351, 1994.
- ²¹Poinsot, T. *et al.*, *Theoretical and Numerical Combustion*, R. T. Edwards, 2001.
- ²²Ferziger, J. H., *Large eddy simulations of turbulent flows*, AIAA Journal, Vol. 15, No. 9, pp. 1261-1267, 1977.
- ²³Sagaut, P., *Large Eddy Simulation for incompressible flows*, New York, Springer, 2001.
- ²⁴Pope, S. B., *Turbulent Flows*, Cambridge, UK, Cambridge University Press, 2000.
- ²⁵Chassaing, P., *Turbulence en Mécanique des fluides. Analyse du phénomène en vue de sa modélisation à l'usage de l'ingénieur*, Toulouse, Polytech, 2000.
- ²⁶Smagorinsky, J., *General recirculation experiments with the primitive equations. I. The basic experiment*, Monthly Weather Review, Vol. 91(3), pp. 99-164, 1963.
- ²⁷Moin, P.*et al.*, *A dynamic subgrid-scale model for compressible turbulence and scalar transport*, Physics of Fluids, Vol. A3, pp. 2746-2757, 1991.
- ²⁸Erlebracher, G.*et al.*, *Towards the large eddy simulation of turbulent flows*, Physics of Fluids, Vol. 238, pp. 155, 1992.
- ²⁹Ducros, F.*et al.*, *Large-eddy simulation of transition to turbulence in a boundary layer over an adiabatic flat plate*, Journal of Fluid Mechanics, Vol. 326, 1996, pp. 1-36, 1996.
- ³⁰Comte, P.*et al.*, *New tools in Turbulence Modelling. Vortices in incompressible LES and non-trivial geometries*, Course of Ecole de Physique des Houches, Springer-Verlag, France, 1996.
- ³¹Lilly, D. K., *A proposed modification of the germano sub-grid closure method*, Physics of Fluids, Vol. A4, 3, pp. 633-635, 1992.
- ³²Germano, M., *Turbulence: The filtering approach*, Journal of Fluid Mechanics, Vol. 238, pp. 238-325, 1992.
- ³³Meneveau, C. *et al.*, *A lagrangian dynamic subgrid-scale model of turbulence*, Journal of Fluid Mechanics, Vol. 319, pp. 353-385, 1996.
- ³⁴Ghosal, S. *et al.*, *A dynamic localization model for large eddy simulation of turbulent flow*, Journal of Fluid Mechanics, Vol. 286, pp. 229-255, 1995.
- ³⁵Williams, F. A., *Combustion theory*, New-York, Benjamin Cummings, 1985.
- ³⁶O. Colin *et al.*, *A thickened flame model for Large Eddy Simulations of turbulent premixed combustion*, Physics of Fluids, 12(7):1843-1863, 2000.
- ³⁷Hunt *et al.*, *Eddies, streams; and convergence zones in turbulent flows*, In Proc. Summer Program, NASA Ames, Stanford, CA, Center for Turbulence Research, 1988.

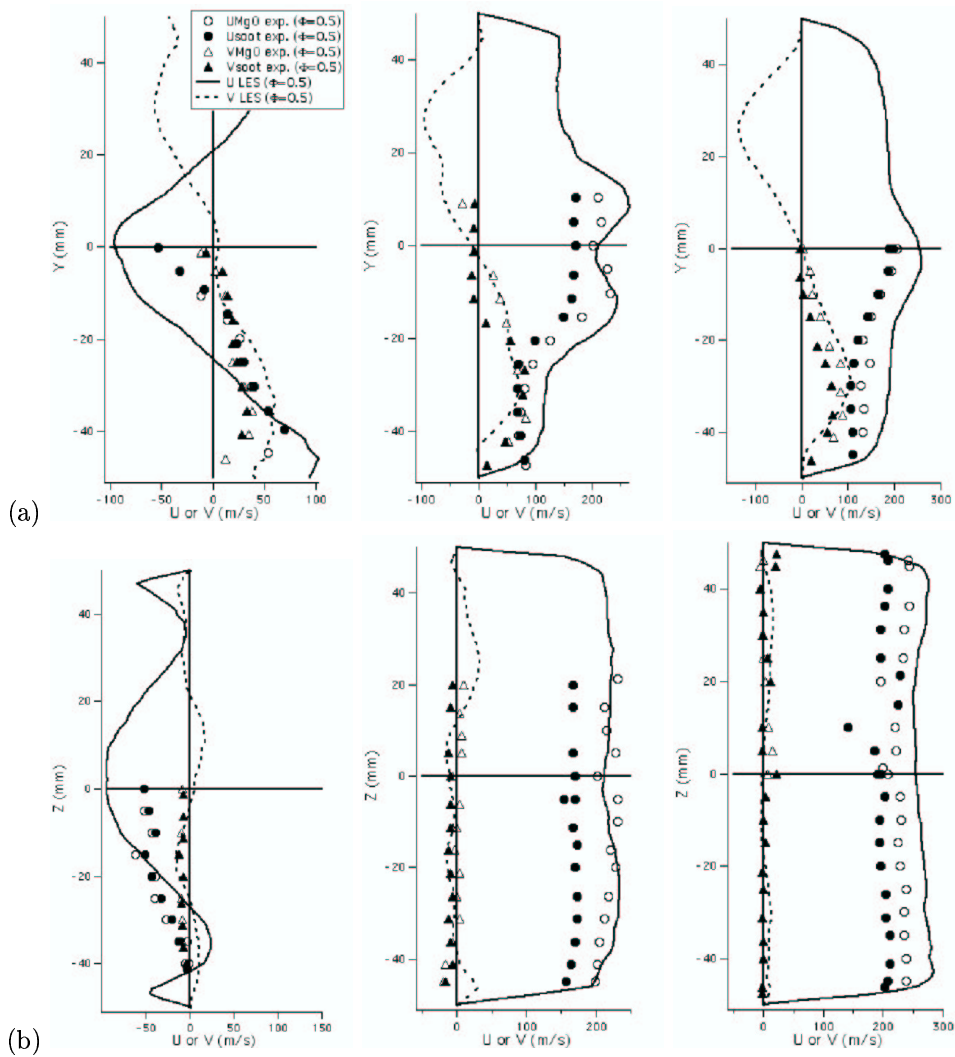


Figure 5. Comparisons between the LES predictions and the experimental measurements for the ramjet dump combustor operating at $\Phi = 0.5$: (a) $y = 0$ and (b) $z = 0$, each column corresponding to the stream-wise locations, $x = 148, 250$ and 336 mm from the end-wall of the main duct.

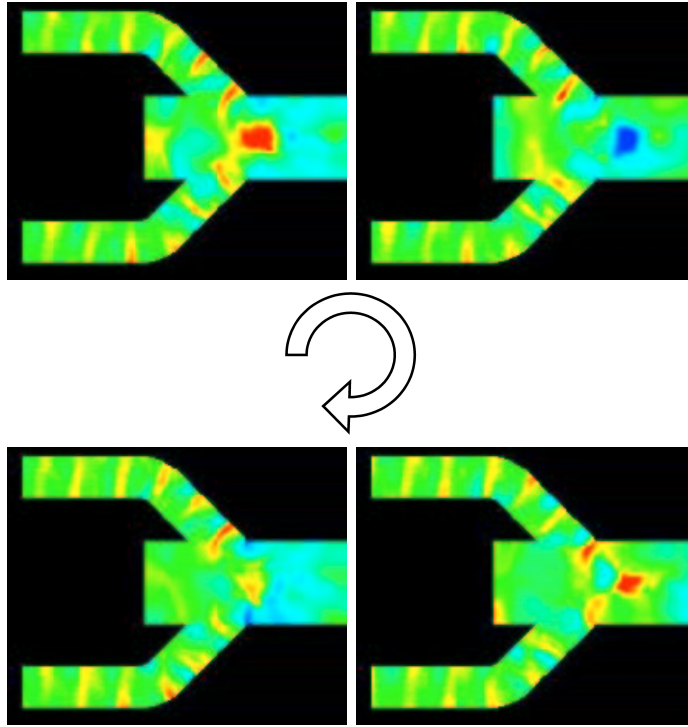


Figure 6. Instantaneous pressure fields as obtained by the reacting LES for an equivalence ratio of 0.75.